

# Determination of Silver in Geological Samples Using Aerosol Dilution ICP-MS After Water-bath Extraction with Inverse Aqua Regia

Yan Wu,<sup>a</sup> Dingming Huang,<sup>a</sup> Tong Feng,<sup>a</sup> Lanlan Jin,<sup>a,\*</sup> Dan Xiong,<sup>b,\*</sup> Jie Yu,<sup>a</sup> Qian Xu,<sup>a</sup> Ruimin Huang,<sup>c</sup> and Shenghong Hu<sup>a</sup>

<sup>a</sup>State Key Laboratory of Biogeology and Environmental Geology, School of Earth Sciences, China University of Geosciences, Wuhan 430074, P.R. China

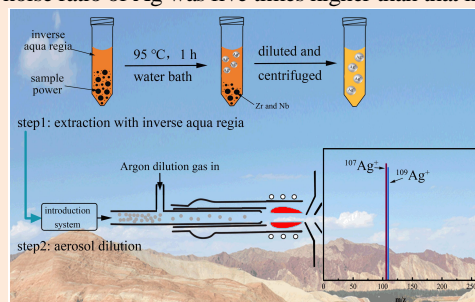
<sup>b</sup>Suizhou Center for Disease Control and Prevention, Suizhou 441300, P.R. China

<sup>c</sup>Institute of Agricultural Quality Standards and Testing Technology Research, Fujian Academy of Agricultural Sciences, Fujian Key Laboratory of Quality and Safety of Agri-Products, Fuzhou 350003, P.R. China

*Received: August 25, 2021; Revised: October 01, 2021; Accepted: October 01, 2021; Available online: October 22, 2021.*

**DOI: 10.46770/AS.2021.906**

**ABSTRACT:** A valid method for trace silver (Ag) detection in geological samples was developed in this study using aerosol dilution inductively coupled plasma-mass spectrometry after extraction with inverse aqua regia. This was proposed primarily to reduce the interference from Nb and Zr during mass spectrometric measurements. Almost 93% of Nb and Zr was removed after the extraction. By mixing an appropriate amount of Ar with the sample aerosol using an aerosol dilution system prior to plasma, the residual Nb oxides and Zr oxides or hydroxides could be successfully removed. The relative yields of the interfering oxides and hydroxides were as low as 0.087% (NbO/Nb) and 0.013% (ZrOH/Zr), which were 3–5 times lower than those in the traditional mode without the addition of Ar. Moreover, the signal-to-noise ratio of Ag was five times higher than that in the traditional mode. The proposed method was applied to the determination of Ag in 68 standard reference materials (SRMs) of soil, sediment, and rock. The results for 47 of these geological SRMs were in good agreement with the reference values. The Ag levels in three SRMs (GSP-2 Granodiorite, STM-2, and SGR-1b) are being reported for the first time herein. For these SRMs, 10 separate aliquots of the sample were digested and analyzed over a period of three months, and analysis revealed that the determined values were reasonable. Thus, the proposed method shows significant potential for the accurate determination of trace Ag in various geological samples.



## INTRODUCTION

Ag is an important indicator in geochemical research as it facilitates the exploration of geochemical anomalies of precious and non-ferrous metals and aids in understanding the enrichment and variation of elements and the origin of deposits, establishing geological prospecting criteria, and assessing mineral resources.<sup>1,2</sup> Therefore, accurate determination of silver (Ag) content in geochemical samples is important. However, Ag is usually present in low concentrations in geological samples except Ag deposits. The average abundance of Ag in the earth's crust is only 0.056  $\mu\text{g g}^{-1}$ , and hence, the accurate quantification of Ag is extremely difficult.<sup>2</sup>

Various atomic spectrometric techniques, including flame atomic absorption spectrometry,<sup>3,4</sup> graphite furnace atomic absorption spectrometry,<sup>5-7</sup> electrothermal atomic absorption spectrometry,<sup>8,9</sup> emission spectrometry,<sup>10-12</sup> inductively coupled plasma optical emission spectrometry,<sup>13-16</sup> microwave plasma atomic emission spectrometry,<sup>17</sup> and inductively coupled plasma-mass spectrometry (ICP-MS),<sup>18-20</sup> have been used for Ag detection in different samples.

ICP-MS is highly sensitive and selective for the determination of trace elements;<sup>21-23</sup> hence, it is also preferred for the determination of trace Ag. The determination of trace Ag by ICP-MS suffers from the interference of polyatomic ions of Nb,

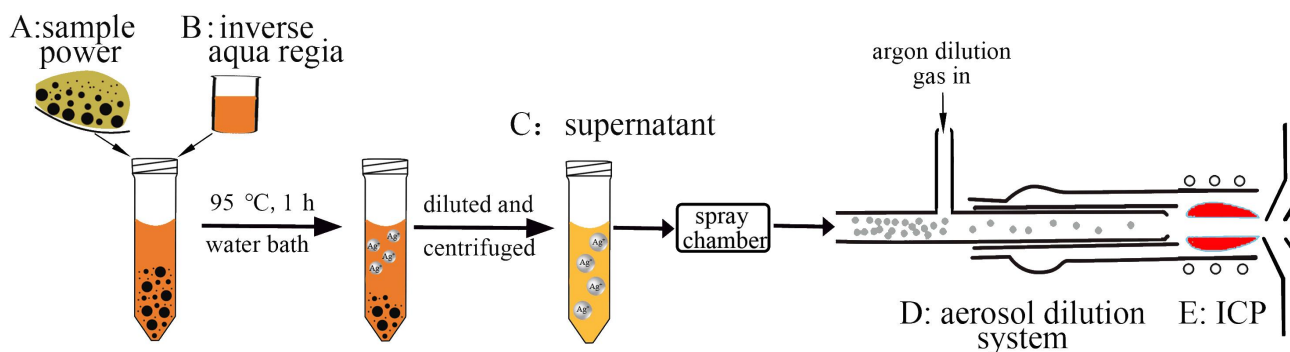


**Fig. 1** Schematic diagram of aerosol dilution ICP-MS after extraction with inverse aqua regia: (A) homogenized sample powder (200 mesh); (B) inverse aqua regia solution (HNO<sub>3</sub>: HCl= 3:1); (C) supernatant; (D) aerosol dilution system; (E) ICP.

Zr, Mo, and Y; for example,  $^{107}\text{Ag}$  interferes with  $^{90}\text{Zr}^{16}\text{OH}^+$ ,  $^{91}\text{Zr}^{16}\text{O}^+$ , and  $^{89}\text{Y}^{18}\text{O}^+$ , while  $^{109}\text{Ag}$  interferes with  $^{93}\text{Nb}^{16}\text{O}^+$ ,  $^{92}\text{Zr}^{16}\text{OH}^+$ , and  $^{92}\text{Mo}^{16}\text{OH}^+$ . In particular, the abundances of Nb, Zr, Mo, and Y in the continental crust are 150-fold, 2300-fold, 14-fold, and 340-fold higher, respectively, than that of Ag (Nb =  $12 \mu\text{g g}^{-1}$ , Zr =  $193 \mu\text{g g}^{-1}$ , Mo =  $1.1 \mu\text{g g}^{-1}$ , and Y =  $21 \mu\text{g g}^{-1}$ ), leading to erroneous results for trace Ag detection in geological samples.<sup>1</sup>

To eliminate the spectral interference in the determination of Ag by ICP-MS, a series of methods have been employed, including the incorporation of correction formulae;<sup>24</sup> preconcentration and separation with P507 resin,<sup>25</sup> thiourea resin,<sup>26,27</sup> and chitosan-based chelating resin;<sup>28</sup> use of extraction technologies for sample digestion;<sup>29–32</sup> development of membrane desolvation and sample introduction techniques;<sup>33</sup> and conducting ion-molecule reactions in a dynamic reaction cell (DRC).<sup>34,35</sup> These techniques can measure the Ag content accurately to some extent; however, these separation methods either cannot eliminate the interference completely, or are time-consuming, or require special instrumental setups or expensive equipment. An online dilution technology, in which the sample aerosol was diluted online with Ar before it entered the plasma, has been used to suppress oxide formation. When a dilution gas was added, the aerosol entering the plasma contained much less water and acid, resulting in more robust plasma and ten times lower oxide formation, which will not significantly compromise the detection limits. This technique has been applied to the analysis of trace elements in complex matrices, without the involvement of complex preprocessing.

The main purpose of this work was to develop a valid method for the determination of trace Ag in geological samples. for the determination of trace Ag in geological samples. Water-bath extraction with inverse aqua regia and online aerosol dilution ICP-MS were combined to eliminate complex interferences from the polyatomic Zr and Nb species. After optimizing the parameters of this method, a series of 68 geological standard reference materials (SRMs) of different types were examined to evaluate the performance of this method in detail.

**Table 1.** Typical Parameters of the ICP-MS System

Parameters	Value
RF power, W	1450
Nebulizer gas flow, Lmin <sup>-1</sup>	0.25
Dilution gas flow, Lmin <sup>-1</sup>	0.85
Sampling depth, Lmin <sup>-1</sup>	8.0
Sweeps per reading, ms	25
Reading per replicate	3
$^{156}\text{CeO}/^{140}\text{Ce}$ ratio, %	Aerosol dilution model < 0.3 Standard model < 3
Isotopic monitored	$^{109}\text{Ag}$

## Experimental

**Analytical Instrumentation.** An Agilent 7700x ICP-MS (Agilent Technologies, USA) instrument equipped with an aerosol dilution system (Fig. 1), a MicroMist nebulizer, and a Peltier-cooled (2°C) quartz Scott-type double-pass spray chamber was used for this work. The operating parameters for ICP-MS were optimized with a tuning solution ( $1.0 \text{ ng mL}^{-1}$  of Ce, Co, Li, Mg, Tl, and Y) prior to determination to obtain the maximum signal intensities and the minimum oxide formation rate ( $\text{CeO}^+/\text{Ce}^+$ ) and doubly charged ratio ( $\text{Ce}^{2+}/\text{Ce}^+$ ). The typical instrumental operating conditions and measurement parameters are listed in Table 1.

**Reagents.** All blanks, standards, and samples were prepared using  $18.2 \text{ M}\Omega \text{ cm}$ -ultrapure water produced by a water purification system (90005-02, LabconcoWaterPro PS, USA). Ultra-pure hydrochloric acid (HCl) and nitric acid (HNO<sub>3</sub>) were prepared from guaranteed grade reagents (Alfa Aesar Ltd., Tianjin) using a two-bottle Teflon sub-boiling distillation system (Saville Corporation, USA). Single-element stock solutions (Cd, Ag, Zr, Nb, and Rh) were purchased from the National Center for Analysis and Testing of Steel Materials (Beijing, P.R. China). The accuracy of the method was assessed using 11 geological SRMs from the United States Geological Survey and 58 SRMs from the Institute of Geophysical and Geochemical Prospecting (P.R. China).

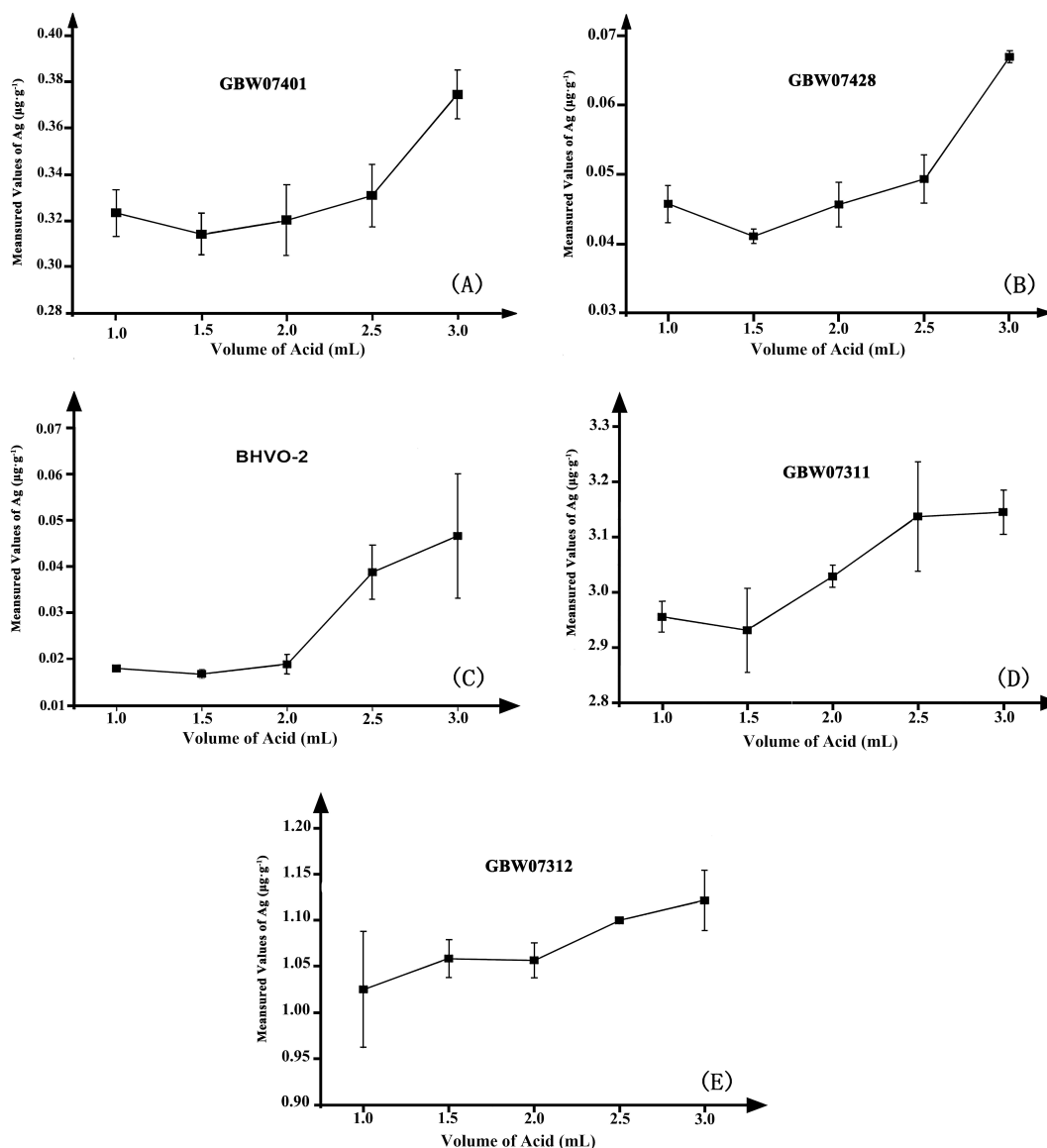


Fig. 2 Effect of inverse aqua regia volume on Ag levels.

Table 2. Ag Levels in 5 Geological SRMs at Different Bath Temperatures (μg g⁻¹)

Reference Materials	Measured Values			Reference Values
	65 °C	65 °C	95 °C	
GBW07304	0.069	0.078	0.076	0.084
GBW07312	1.05	1.12	1.11	1.15
GBW07447	0.067	0.063	0.066	0.066
GBW07457	0.1	0.11	0.11	0.13
GBW07121	0.022	0.024	0.024	0.03

**Sample Pretreatment.** A homogenized sample powder (200 mesh, 0.2000 g) was weighed into a 10 mL polyethylene centrifuge tube, and 3.0 mL of freshly prepared inverse aqua regia solution (HNO<sub>3</sub>: HCl = 3:1) was added. The centrifuge tube was then placed in a water bath at 95 °C for 1 h. After cooling to about 25 °C, the sample solution was diluted to 10 mL with high-purity water and centrifuged to remove the undissolved

solid particles. Two milliliters of the supernatant were transferred to a new polyethylene tube and diluted with high-purity water to 6 mL (Fig. 1). For comparison, two conventional digestion methods, namely, closed pressurized digestion with a mixture of HF and HNO<sub>3</sub> and electric heating plate digestion with aqua regia, were also used.

## RESULTS AND DISCUSSION

**Optimization of digestion conditions.** During sample digestion, the amount of inverse aqua regia directly affects the recovery of the target elements and interfering elements. Five reference materials (GBW07401, GBW07428, GBW07311, GBW07312, and BHVO-2) were used to optimize the dosage of inverse aqua regia. Fig. 2 shows that the recovery of Ag increased with the volume of inverse aqua regia. Five milliliters of inverse aqua

**Table 3. Signal Intensity from Ag, Nb, Zr at m/z = 109**

	Signal Intensity / cps at m/z = 109			SBR
	Ag (1 ng mL <sup>-1</sup> )	Nb (200 ng mL <sup>-1</sup> )	Zr (2000 ng mL <sup>-1</sup> )	
<b>Standard Model</b>	11224.6	17330.1	3866.1	0.53
<b>Aerosol Dilution Model</b>	2275.8	738.7	247.2	2.31

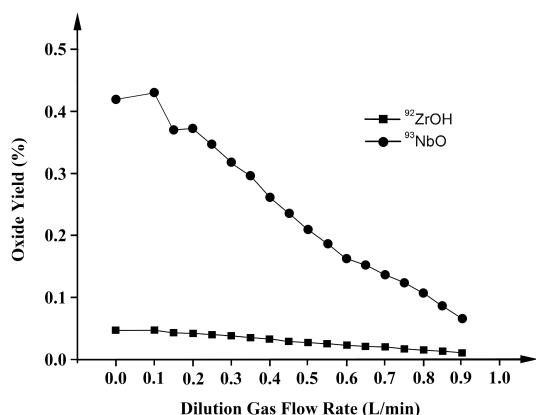


**Fig. 3** Effect of the flow rate of dilution gas on oxide formation ratios (ZrOH<sup>+</sup>/Zr<sup>+</sup>, NbO<sup>+</sup>/Nb<sup>+</sup>).

regia were used; the Ag content determined was consistent with the recommended value, while the recovery of Nb was lower than 7%. Thus, 3mL of inverse aqua regia was sufficient to dissolve Ag effectively from the sample; the interfering elements were not extracted, and the separation from the interfering elements was ascertained.

The effect of water bath temperature on the recovery of Ag was also investigated using five reference materials (GBW07447, GBW07457, GBW07304, GBW07312, and GBW07121). Digestion experiments were carried out at three temperatures (25 °C, 65 °C, and 95 °C), and the errors between the measured values and the recommended values of Ag in these five reference

materials were compared. Although the measured values of Ag in these five reference materials were within the acceptable error range at the three water bath temperatures, the measured values were closer to the recommended values at higher temperatures (65 °C and 95 °C) (Table 2). Therefore, the accuracy of Ag detection can be improved by increasing the water bath temperature, although there is no obvious relationship between these two factors. To ensure reliability of the analysis results, Ag was extracted from the samples at a water bath temperature of 95 °C for 1 h.

#### Elimination of interference from polyatomic ions.

Interferences in the determination of Ag in geological samples using ICP-MS are mainly from the Zr-containing (<sup>90</sup>ZrOH, <sup>91</sup>ZrO, <sup>92</sup>ZrOH) and Nb-containing (<sup>93</sup>NbO) polyatomic ions. The aerosol dilution technique, in which an aerosol sample is diluted online with Ar prior to plasma, can minimize the interference from complex matrices (such as high-salt samples) on target elements and also the interference caused by liquid dilution by reducing the sample aerosol density in real time. More importantly, this online aerosol dilution technique can reduce the amount of water and acid entering the ICP. This not only maintains the high temperature of the ICP but also significantly minimizes the formation of interference ions such as oxides and other polyatomic ions. In this study, the aerosol dilution technique was used to reduce the interference of <sup>92</sup>ZrOH and <sup>93</sup>NbO. Fig. 3 shows the relationship between ZrOH<sup>+</sup>/Zr<sup>+</sup>, NbO<sup>+</sup>/Nb<sup>+</sup>, and the flow rate of the dilution gas. The ZrOH<sup>+</sup>/Zr<sup>+</sup> and NbO<sup>+</sup>/Nb<sup>+</sup> ratios decreased with increasing flow rate of the dilution gas. When this flow rate was 0.85 L/min, the two ratios decreased by 3–5 times compared with those in the traditional ICP-MS mode (ZrOH<sup>+</sup>/Zr<sup>+</sup> = 0.013%, NbO<sup>+</sup>/Nb<sup>+</sup> = 0.087%).

Table 3 shows a comparison of the signal intensity and signal background ratio (SBR) of the traditional and aerosol dilution modes in ICP-MS, based on the simulated abundances of the

**Table 4. Ag Levels in 5 Geological SRMs Determined Using this Method (n = 10, µg g<sup>-1</sup>)**

SRMs	GBW07402	GBW07456	GBW07359	GBW07360	GBW07105
<b>Measured Values</b>	0.066	0.138	0.048	0.781	0.031
	0.057	0.179	0.047	0.752	0.027
	0.063	0.156	0.048	0.735	0.029
	0.056	0.154	0.043	0.834	0.034
	0.051	0.154	0.054	0.815	0.024
	0.052	0.168	0.048	0.682	0.033
	0.051	0.171	0.050	0.770	0.030
	0.055	0.147	0.043	0.761	0.033
	0.058	0.150	0.048	0.809	0.030
	0.052	0.160	0.053	0.738	0.044
<b>Average Values</b>	0.056±0.005	0.16±0.01	0.048±0.003	0.77±0.04	0.032±0.005
<b>RSD, %</b>	8.9	7.5	6.3	5.6	15.6
<b>Reference Values</b>	0.054±0.007	0.14±0.01	0.050±0.007	0.74±0.14	0.040±0.008

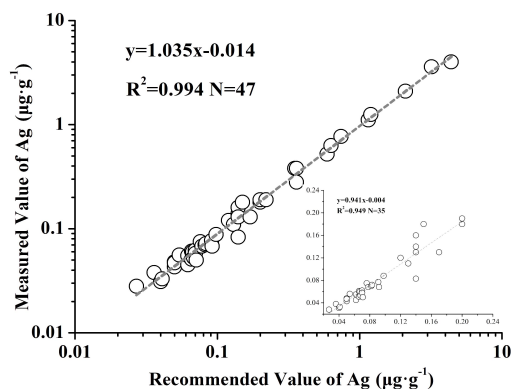


**Fig. 4** Ag values determined for 47 geological SRMs using the proposed method as a function of their certified values. The inset shows the values for the geological SRMs containing ultra-trace levels of Ag (<0.2 µg·g<sup>-1</sup>).

interfering elements (Zr: 2000 ng mL<sup>-1</sup>, Nb: 200 ng mL<sup>-1</sup>) and Ag (1 ng mL<sup>-1</sup>) in continental crust. In the traditional mode, the signal response intensities of Ag, Nb, and Zr at m/z 109 were 11224.6, 17330.1, and 3866.1 cps, respectively, and the SBR was 0.53. In the aerosol dilution mode, the corresponding signal response intensities were 2275.8, 738.7, and 247.2, respectively, while the SBR was 2.31. Although the signal intensity of Ag in the aerosol dilution mode was reduced by five times, the SBR increased by five times, which was more conducive for the accurate detection of Ag.

**Analysis procedure.** The standard solution of Ag was diluted with 2% nitric acid to obtain a series of standard solutions with concentrations of 0, 0.1, 1, 10, and 100 ng mL<sup>-1</sup>. The working curve of Ag was obtained under the optimal working conditions. The detection limit of this method was 1.1 ng g<sup>-1</sup> (considering a 300-fold dilution factor), which was 10 times the standard

**Table 5.** Ag Levels in 69 Geological SRMs Determined Using this Method (µg g<sup>-1</sup>)

	Sample Name	Character	Measured Values	Reference Values
Soils	GBW07401	Dark brown soil	0.38±0.028	0.35±0.05
	GBW07402	Chestnut soil	0.056±0.005	0.054±0.007
	GBW07403	Yellow brown soil	0.077±0.009	0.091±0.007
	GBW07404	Weathered limestone soil	0.045±0.005	0.07±0.011
	GBW07405	Yellow red soil	4.0±0.56	4.4±0.4
	GBW07406	Yellow red soil	0.18±0.015	0.2±0.02
	GBW07423	Tillage soil	0.075±0.006	0.076±0.013
	GBW07424	Tillage soil	0.072±0.008	0.083±0.01
	GBW07425	Tillage soil	0.088±0.006	0.098±0.007
	GBW07426	Tillage soil	0.068±0.008	0.078±0.007
	GBW07427	Tillage soil	0.060±0.004	0.067±0.006
	GBW07428	Tillage soil	0.051±0.004	0.084±0.007
	GBW07429	Tillage soil	0.18±0.015	0.15±0.02
	GBW07430	Tillage soil	0.14±0.002	0.14±0.02
	GBW07446	Sandy soil	0.028±0.003	0.050±0.006
	GBW07447	Saline-alkali soil	0.051±0.006	0.066±0.005
	GBW07448	Brown desert soil	0.043±0.004	0.050±0.005
	GBW07449	Saline-alkali soil	0.053±0.007	0.068±0.007
	GBW07450	Sierozem soil	0.036±0.004	0.073±0.003
	GBW07451	Beach sediments	0.044±0.004	0.074±0.006
	GBW07453	Beach sediments	0.052±0.004	0.092±0.013
	GBW07454	Loess	0.062±0.007	0.070±0.008
	GBW07455	Sediment of Huaihe River	0.058±0.004	0.070±0.004
	GBW07456	Yangtze River Sediments	0.16±0.01	0.14±0.01
	GBW07457	Sediment of Xiangjiang River	0.11±0.01	0.13±0.01
	GBW07302	Stream sediment	0.061±0.007	0.066±0.010
	GBW07303	Stream sediment	0.52±0.04	0.59±0.05
	GBW07305	Stream sediment	0.28±0.02	0.36±0.03
	GBW07306	Stream sediment	0.38±0.03	0.36±0.03
	GBW07309	Stream sediment	0.061±0.009	0.089±0.010
	GBW07310	Stream sediment	0.055±0.007	0.27±0.02
Stream sediments	GBW07311	Stream sediment	3.6±0.15	3.2±0.4
	GBW07301a	Stream sediment	0.038±0.007	0.036±0.010

Rocks	GBW07303a	Stream sediment	0.19±0.01	0.20±0.02
	GBW07304a	Stream sediment	0.19±0.008	0.22±0.03
	GBW07305a	Stream sediment	0.63±0.06	0.63±0.06
	GBW07307a	Stream sediment	1.25±0.09	1.20±0.08
	GBW07308a	Stream sediment	0.12±0.01	0.12±0.02
	GBW07312	Stream sediment	1.11±0.09	1.15±0.11
	GBW07317	Stream sediment	0.013±0.003	0.027±0.005
	GBW07358	Stream sediment	0.13±0.009	0.14±0.01
	GBW07359	Stream sediment	0.048±0.003	0.050±0.007
	GBW07360	Stream sediment	0.77±0.04	0.74±0.14
	GBW07361	Stream sediment	0.015±0.003	0.044±0.014
	GBW07362	Stream sediment	0.068±0.005	0.092±0.005
	GBW07363	Stream sediment	0.070±0.003	0.082±0.008
	GBW07364	Stream sediment	0.083±0.006	0.14±0.01
	GBW07365	Stream sediment	0.044±0.01	0.068±0.010
	GBW07366	Stream sediment	2.1±0.17	2.1±0.3
	GBW07103	Biotite granite	0.014±0.002	0.033±0.007
	GBW07104	Quartz hornblende andesite	0.050±0.008	0.071±0.009
	GBW07105	Olivine basalt	0.031±0.005	0.040±0.008
	GBW07106	Quartz sandstone	0.045±0.006	0.062±0.007
	GBW07107	Shale	0.017±0.003	0.047±0.009
	GBW07108	Argillaceous limestone	0.026±0.004	0.043±0.011
	GBW07121	Granite gneiss	0.019±0.004	0.03±0.01
	GBW07122	Plagioclase amphibolite	0.047±0.005	0.05
	AGV-2	Andesite	0.055±0.004	0.062±0.001
	BCR-2	Basalt	0.033±0.003	0.041±0.004
	BHVO-2	Basalt	0.047±0.016	0.050±0.002
	BIR-1a	Basalt	0.013±0.001	0.036
	DNC-1a	Diabase	0.028±0.003	0.027
	DGPM-1	Gold ore	0.034±0.03	0.79
	NOD-A-1	Manganese nodule	0.13±0.015	0.17
	QLO-1a	Quartz latite	0.018±0.001	0.062
	SGR-1b	Shale	0.15±0.009	/
	GSP-2	Granodiorite	0.084±0.009	/
	STM-2	Syenite	0.082±0.011	/

deviation multiplied by the dilution ratio of the full procedural blank for 11 successive measurements.

Moreover, five geological SRMs (GBW07402, GBW07456, GBW07359, GBW07360, and GBW07105) were assessed for 10 parallel comparative analyses using this method (Table 4). Although Ag is present at ultra-trace levels ( $< 0.20 \mu\text{g g}^{-1}$ ) in these geological SRMs, the determined average values are in agreement with the reference values. The relative standard deviations (RSDs) for 10 parallel comparative analyses were 8.9%, 7.5%, 6.3%, 5.6%, and 15.6% and met the requirements of geochemical sample analysis.

**Analysis of Ag in geological reference materials.** The proposed method was also employed to determine the Ag levels in 68 geological SRMs, comprising 25 soil samples, 24 stream sediment samples, and 19 rock samples. The results obtained and

their certified values are listed in Table S1. The Ag values determined in 18 geological SRMs were lower than the recommended values. Among the 18 SRMs, the recommended Ag values of 15 samples were less than  $0.092 \mu\text{g g}^{-1}$ . If the Ag content in a sample is too low, stable detection signals cannot be obtained by ICP-MS, and this is the primary reason for the large deviation of the results. It is particularly interesting that all the determined values for the 18 SRMs are lower than the recommended values. We speculate that the water-bath extraction method cannot effectively destroy the lattice of some minerals (gold ore, carbonate rock, etc.), because of which Ag in the lattice cannot be completely released; this results in low values. Moreover, for the samples with a high organic content, such as GBW07107 (the organic matter content is 13–20%), the adsorption of organic matter will decrease the extraction efficiency of Ag if organism is not completely removed; this too results in low values. Further studies are required to optimize the



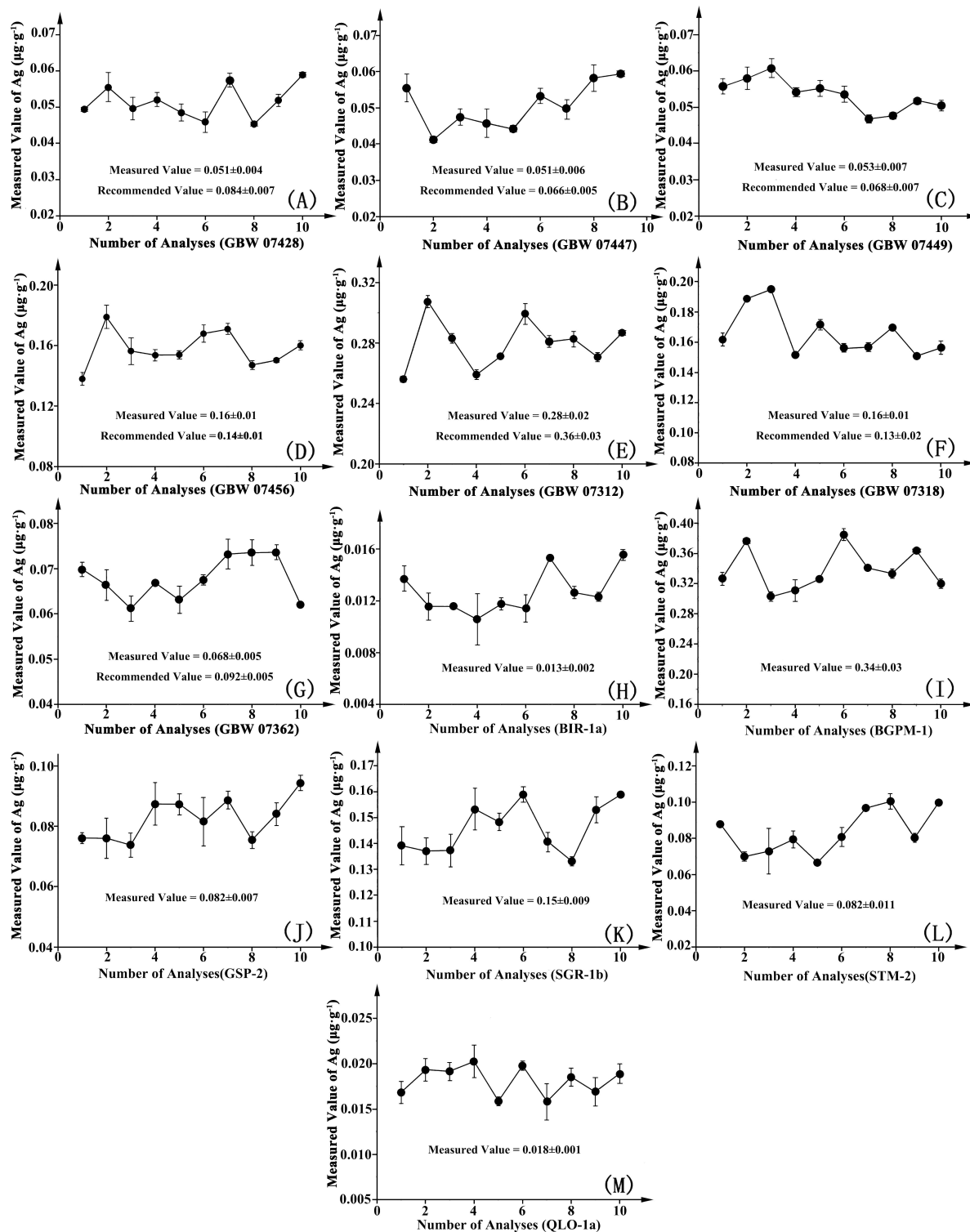


**Fig. 5** Reproducibility of Ag values obtained using the proposed method in 13 geological SRMs: GBW07428 (a), GBW07447 (b), GBW07449 (c), GBW07456 (d), GBW07305 (e), GBW07318 (f), GBW07362 (g), BIR-1a (h), BGPM-1 (i), GSP-2 (j), SGR-1b (k), STM-2 (l), and QLO-1a (m). For each SRM, ten separate aliquots of the samples were analyzed over a period of three months.

efficiency of Ag extraction from different matrix samples.

The measured Ag levels in 47 geological SRMs were essentially

in agreement with their certified values (Fig. 4 and Table 5), while the Ag contents in 35 geological SRMs were less than 0.2  $\mu\text{g g}^{-1}$ . Furthermore, three SRMs (SGR-1b, GSP-2, and STM-2) have no reference or literature values at present and the recommended values of these SRMs are provided in this work. The results of repeated analyses, in which the SRMs were extracted and re-analyzed ten times over a period of three months, were consistent (Fig. 5), indicating that this method is stable, and our recommended values are reliable.

## CONCLUSIONS

A valid method for the determination of trace Ag levels in geological samples using aerosol dilution ICP-MS after extraction with boiling inverse aqua regia was developed. The significant interference from Zr or Nb-based oxides and hydroxides was effectively reduced using the proposed method. Among the 68 geological SRMs examined, the Ag levels determined for 47 samples were in agreement with their certified or literature values. The method reported herein has also been used to determine the Ag levels of three SRMs (GSP-2 Granodiorite, STM-2, and SGR-1b) whose Ag content has not been reported previously. This method has significant potential for the accurate determination of ultra-low levels of Ag ( $<0.2 \mu\text{g g}^{-1}$ ) in various geological samples.

## AUTHOR INFORMATION

### Corresponding Author

\*L. L. Jin

Email address: annjll@163.com

\*D. Xiong

Email address: kirazxxl@163.com

### Notes

The authors declare no competing financial interest.

## ACKNOWLEDGMENTS

The authors are grateful for the financial support from the National Natural Science Foundation of China (41703132, 21565013), the Science and Technology Program of Zhejiang Province (LGC20B050014), and the Basic Scientific Research of Public Interest Research Institutes in Fujian Province (2019R1022-2). The authors thank the State Key Laboratory of Biogeology and Environmental Geology for its support.

## REFERENCES

1. S. Gao, T. C. Luo, B. R. Zhang, H. F. Zhang, Y. W. Han, Z. D. Zhao, and Y. K. Hu, *Geochim. Cosmochim. Acta.*, 1998, **62**, 1959-1975. [https://doi.org/10.1016/S0016-7037\(98\)00121-5](https://doi.org/10.1016/S0016-7037(98)00121-5)
2. R. L. Rudnick, S. Gao, H. D. Holland, and K. K. Turekian, Composition of the continental crust. In: Rudnick RL, editor. The crust. In: Holland HD, Turekian KK, editors. Treatise on Geochemistry Elsevier-Pergamon, 2003.
3. S. Z. Mohammadi, D. Afzali, M. A. Taher, and Y. M. Baghelani, *Talanta*, 2009, **80**, 875-879. <https://doi.org/10.1016/j.talanta.2009.08.009>
4. S. Rastegarzadeh, N. Pourreza, and A. Larki, *J. Ind. Eng. Chem.*, 2015, **24**, 297-301. <https://doi.org/10.1016/j.jiec.2014.09.045>
5. M. Resano, M. Aramend, E. Garc'ia-Ruiz, C. Crespo, and M. A. Belarra, *Anal. Chim. Acta*, 2006, **571**, 142-149. <https://doi.org/10.1016/j.aca.2006.04.037>
6. P. Liang, L. L. Zhang, and E. Zhao, *Talanta*, 2010, **82**, 993-996. <https://doi.org/10.1016/j.talanta.2010.06.004>
7. M. C. Saha, R. Baskey, and S. Lahiri, *Atom. Spectrosc.*, 2015, **36**, 177-181. <https://doi.org/10.46770/AS.2015.04.005>
8. J. L. Manzoori, H. Abdolmohammad-Zadeh, and M. Amjadi, *J. Hazard. Mater.*, 2007, **144**, 458-463. <https://doi.org/10.1016/j.jhazmat.2006.10.084>
9. I. M. Ditter, D. L. G. Borges, B. Welz, A. J. Curtius, and H. t. Becker-Ross, *Microchim. Acta*, 2009, **167**, 21-26. <https://doi.org/10.1007/s00604-009-0211-x>
10. X. M. Zhang and Q. Zhang, *Rock Mineral Anal.*, 2006, **25**, 323-326. <https://doi.org/10.3969/j.issn.0254-5357.2006.04.006>
11. A. I. Kuznetsova, O. V. Zarubina, and O. A. Sklyarova, *Geostand. Geoanal. Res.*, 2009, **31**, 251-259. <https://doi.org/10.1111/j.1751-908X.2007.00831.x>
12. C. D. Cao, Y. Wei, and J. B. Liu, *Rock Mineral Anal.*, 2010, **29**, 458-460. <https://doi.org/10.15898/j.cnki.11-2131/td.2010.04.012>
13. J. P. Bennett, E. Chiriboga, J. Coleman, and D. M. Waller, *Sci. Total Environ.*, 2000, **246**, 261-269. [https://doi.org/10.1016/S0048-9697\(99\)00464-7](https://doi.org/10.1016/S0048-9697(99)00464-7)
14. E. de Miguel, S. Charlesworth, A. Ordonez, and E. Seijas, *Sci. Total Environ.*, 2005, **340**, 137-148. <https://doi.org/10.1016/j.scitotenv.2004.07.031>
15. A. R. Jacobson, M. B. McBride, P. Baveye, and T. S. Steenhuis, *Sci. Total Environ.*, 2005, **345**, 191-205. <https://doi.org/10.1016/j.scitotenv.2004.10.027>
16. M. Hosoba, K. Oshita, R. K. Katarina, T. Takayanagi, M. Oshima, and S. Motomizu, *Anal. Chim. Acta*, 2009, **639**, 51-56. <https://doi.org/10.1016/j.aca.2009.02.050>
17. B. Vysetti, D. Vummiti, P. Roy, C. Taylor, C. T. Kamala, M. Satyanarayanan, P. Kar, K. S. V. Subramanyam, A. K. Raju, and K. Abburi, *Atom. Spectrosc.*, 2014, **35**, 65-78. <https://doi.org/10.46770/AS.2014.02.003>
18. K. Ndung'u, M. A. Ranville, R. P. Franks, and A. R. Flegal, *Mar. Chem.*, 2006, **98**, 109-120. <https://doi.org/10.1016/j.marchem.2005.07.003>
19. Z. C. Wang, H. Becker, and F. Wombacher, *Geostand. Geoanal. Res.*, 2014, **39**, 185-208. <https://doi.org/10.1111/j.1751-908X.2014.00312.x>
20. R. M. Gaschnig, R. L. Rudnick, and W. F. McDonough, *Geostand. Geoanal. Res.*, 2014, **39**, 371-379. <https://doi.org/10.1111/j.1751-908X.2014.00330.x>



21. X. Lin, W. Guo, L. L. Jin, and S. H. Hu, *Atom. Spectrosc.*, 2020, **41**, 1-10. <https://doi.org/10.46770/AS.2020.01.001>
  22. Y. Cui, L. L. Jin, H. L. Li, S. H. Hu, and Y. Lian, *Atom. Spectrosc.*, 2020, **41**, 87-92. <https://doi.org/10.46770/AS.2020.02.006>
  23. W. X. Wang, X. Dai, W. Guo, L. L. Jin, and S. H. Hu, *Atom. Spectrosc.*, 2020, **41**, 74-80. <https://doi.org/10.46770/AS.2020.02.004>
  24. J. Y. Hu, Z. Liu, and H. Z. Wang, *Anal. Chim. Acta*, 2002, **451**, 329-335. [https://doi.org/10.1016/S0003-2670\(01\)01406-4](https://doi.org/10.1016/S0003-2670(01)01406-4)
  25. Z. Xing and L. Qi, *Rock Mineral Anal.*, 2013, **32**, 398-401. <https://doi.org/10.15898/j.cnki.11-2131/td.2013.03.004>
  26. Y. B. Zhang, Z. Z. Cheng, and H. Li, *Chin. J. Anal. Lab.*, 2006, **25**, 105-108. <https://doi.org/10.13595/j.cnki.issn1000-0720.2006.0216>
  27. X. L. Liu, W. J. Sun, T. Y. Wen, T. F. Wang, W. Z. Sun, Y. X. Li, and J. Guo, *Chin. J. Anal. Chem.*, 2015, **43**, 1371-1376. <https://doi.org/10.11895/j.issn.0253-3820.150382>
  28. R. K. Katarina, T. Takayanagi, M. Oshima, and S. Motomizu, *Anal. Chim. Acta*, 2006, **558**, 246-253. <https://doi.org/10.1016/j.aca.2005.11.010>
  29. L. P. Zhou and Z. X. Li, *Chin. J. Anal. Lab.*, 2005, **24**, 20-25. <https://doi.org/10.13595/j.cnki.issn1000-0720.2005.0203>
  30. C. Y. Sun, X. F. Dai, X. L. Dai, B. Chen, and C. J. Zheng, *Rock Mineral Anal.*, 2015, **34**, 292-296. <https://doi.org/10.15898/j.cnki.11-2131/td.2015.03.005>
  31. L. Strnad, O. Sebek, M. Fayadov, and J. Vrba, *Geostand. Geoanal. Res.*, 2015, **40**, 257-266. <https://doi.org/10.1111/j.1751-908X.2015.00368.x>
  32. Y. Wang, L. A. Baker, and I. D. Brindle, *Talanta*, 2016, **148**, 419-426. <https://doi.org/10.1016/j.talanta.2015.11.019>
  33. J. Xu, Z. C. Hu, Y. S. Liu, S. H. Hu, H. L. Yuan, and S. G., *Chin. J. Anal. Chem.*, 2008, **36**, 1493-1498. <https://doi.org/10.3321/j.issn:0253-3820.2008.11.008>
  34. W. Guo, S. H. Hu, J. Y. Zhang, and H. F. Zhang, *Sci. Total Environ.*, 2011, **409**, 2981-2986. <https://doi.org/10.1016/j.scitotenv.2011.04.011>
  35. J. L. Xu, X. Xing, R. L. Tang, M. Y. Hu, P. P. Zhang, J. F. Bai, and Q. Zhang, *Rock Mineral Anal.*, 2019, **38**, 394-402. <https://doi.org/10.15898/j.cnki.11-2131/td.201812070131>
-